# ON THE IMPORTANCE OF THE DOUBLE PENGUIN-LIKE DIAGRAMS FOR THE ε PARAMETER IN THE STANDARD MODEL

J.O. EEG
*Institute of Physics, University of Oslo, N-1000 Oslo, Norway*

and

I. PICEK [1,2,3]
*DESY, D-2000 Hamburg, Fed. Rep. Germany*

Received 13 May 1986; revised manuscript received 16 June 1986

We calculate box diagrams of penguin variety which represent additional short-distance contribution to the $K^0$–$\bar{K}^0$ mixing. Its imaginary part is sizeable and leads to an extra contribution to the *CP*-violating parameter $\epsilon$, which lowers substantially (by 25%) the value given by the standard box.

*1. Introduction.* The $K^0$–$\bar{K}^0$ mixing represents an exquisitely sensitive channel for improvement of our knowledge of *CP* violation. Accordingly, our consideration is based on the basic features of *CP* violation in the *minimal standard model* (SM):
- *CP* violation appears only as a loop effect;
- its measure, represented by the parameter $\epsilon$, seems to come mainly from the short distance (SD) physics.

These features have motivated us to examine the SD $K^0$–$\bar{K}^0$ mixing mechanisms in detail. In particular, we want to invoke diagrams of a different topological structure than the box diagram usually considered. We illustrate both the possibility of new important contributions from these diagrams and the necessity for going beyond the leading log approximation used so far.

Recently there has been considerable interest in the so-called "*double-penguin-diagram*" (DP) contribution to the local four-quark $\Delta S=2$ hamiltonian [1–3]. The estimate of ref. [1], based on a simplified treatment of a single diagram shown in fig. 1, gave a large $K_L$–$K_S$ mass difference proportional to $m_t^2$. The doubt cast on this result by ref. [2] initiated the "double-penguin controversy" [4]. Our previous paper [3] settled this controversy by an improved SD treatment which included

(i) the momentum dependence of the penguin loop and the "non-leading" terms,

(ii) the non-local part (corresponding to the $p_\mu p_\nu/p^2$ term in the penguin-gluon propagator),

(iii) all (four) QCD gauge-independent diagrams of fig. 1.

As a result, the set of diagrams in fig. 1 turns out to be negligible in comparison with the simplest "standard box" diagram of Gaillard and Lee [5].

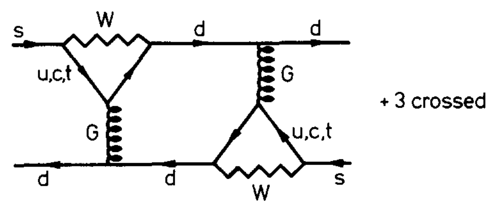


Fig. 1. A typical double penguin diagram, which has three crossed diagram companions.

[1] A. von Humboldt fellow.
[2] On leave of absence from the Rudjer Bosković Institute, Zagreb, Croatia, Yugoslavia.
[3] Supported in part by the NSF YOR 84/078 grant.



0370-2693/86/$ 03.50 © Elsevier Science Publishers B.V. (North-Holland Physics Publishing Division)

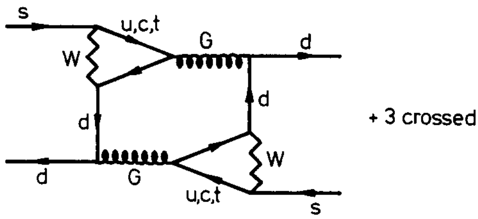


Fig. 2. Annihilation channel counterpart of fig. 1.

However, the ratio of the double penguin over the standard box, becomes slightly modified (by a factor 0.85) when we include

(iv) both exchange (fig. 1) and annihilation (fig. 2) diagrams, as it will be done systematically in the present paper. Based on the experience gained in our previous penguin-loop calculations of *CP*-violating amplitudes [6], we conjectured in ref. [3] about possible new important contributions to the *CP*-violating parameter $\epsilon$. Here we demonstrate how this conjecture is actually realized. We will not go into all details in this short letter, but will rather proceed directly to describe the main results.

2. *Full set of three-loop ($\sim \alpha_s^2 G_F^2$) diagrams.* A nice feature of the set of diagrams shown in fig. 1 is its gauge independence, as a consequence of each gluon being accompanied with a transverse projector

$$P^{\alpha}_{T\rho} p^{-2}(g^{\rho\beta} - \xi p^{\rho} p^{\beta}/p^2) = g^{\alpha\beta} - p^{\alpha}p^{\beta}/p^2 \ .$$

The projector $P_T$ appears in the expression for the penguin-loop transition $s \to dG$:

$$f_P C(p^2, m^2, M^2) \bar{d}\gamma_\alpha t^a L s P^{\alpha}_{T\rho}(p) \ , \tag{1a}$$

where

$$f_P = -\tfrac{1}{3}\sqrt{2}\, G_F g_s / 4\pi^2 \ ,$$

$$C(p^2, m^2, M^2) = 6 \int_0^1 dx\, x(1-x) \ln \frac{M^2 + p^2 x(1-x)}{m^2 + p^2 x(1-x)} \tag{1b}$$

and $(m, M)$ refers to either $(m_u, m_c)$ or $(m_c, m_t)$ pairs of current quark masses. The nice feature of *explicit gauge independence* is already lost in simplest extension to the set of diagrams shown in fig. 3. If at these diagrams the gluon line not attached to the penguin loops is removed, then one ends up with the gauge-independent "siamese-penguin mechanism" [7]. However, the explicit (although model-dependent) evaluation [7] of this mechanism shows that its contribution to the $K^0$–$\bar{K}^0$ mixing is entirely negligible. Thus we are back to the "siamese penguin-box" diagrams (SP) (fig. 3), the estimate of which will be more straightforward, but requires other accompanying diagrams to maintain gauge independence.

One of such additional diagrams we promised to consider [3] is the "*diamond box*" (D) (fig. 4). It involves a triangle loop for the $s \to dGG$ transition (fig. 5):

$$f_t \bar{d}\, t^b t^a \gamma^\alpha T_{\alpha\rho\sigma} L s \ , \quad f_T = 2\sqrt{2}\, G_F \alpha_s / 4\pi \ . \tag{2}$$

The tensor in (2) is the sum of the symmetric and antisymmetric part of the following structure:

$$T^S_{\alpha\rho\sigma} = A(g_{\alpha\sigma} p_\rho + g_{\alpha\rho} p_\sigma) + B g_{\rho\sigma} p_\alpha + C p_\alpha p_\rho p_\sigma \ , \tag{3a}$$

and

$$T^A_{\alpha\rho\sigma} = -\mathrm{i} F \epsilon_{\alpha\rho\sigma\lambda} p^\lambda \ . \tag{3b}$$

For expository purposes, it is convenient to restrict oneself to the leading-log part (contained only in the functions $A$ and $B$, whose complete form will be presented elsewhere):

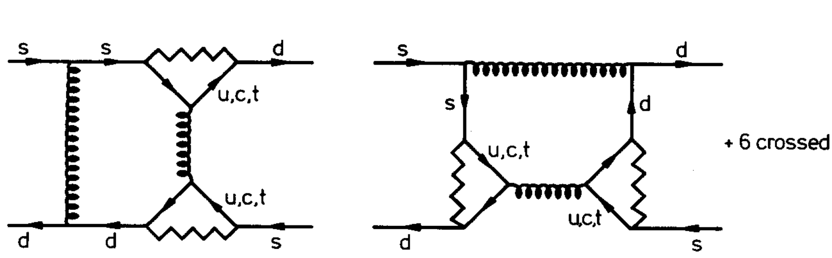


Fig. 3. Example of QCD gauge dependent double penguin diagram (siamese-penguin box).

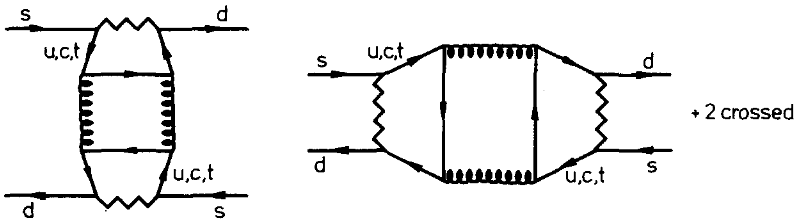


Fig. 4. Diamond box, another gauge dependent diagram of order $\alpha_s^2 G_F^2$.

$$\sqrt{2}\, G_F(\alpha_s/3\pi)\ln(M^2/p^2)\, \bar{d}\, t^b t^a$$
$$\times[-p_\rho\gamma_\sigma - p_\sigma\gamma_\rho + 2g_{\rho\sigma}p_\alpha\gamma^\alpha]Ls\,. \quad (4)$$

Once being equipped with the penguin (1) and triangle (2) loop subdiagrams, we complete the list of diagrams of order $\alpha_s^2 G_F^2$ by considering also the "mixed penguin" box diagrams (MP) (fig. 6). In order to demonstrate the completeness (i.e. gauge invariance), let us write down the listed box subsets in terms of the leading-log expression (with the colour and Dirac algebra factors extracted)

$$\tilde{M}_{\text{l-log}} = (\bar{d}\gamma_\mu Ls)^2 (2\sqrt{2}\, G_F)^2 \frac{1}{16\pi^2}$$
$$\times \int dp^2 \left(\frac{\alpha_s(p^2)}{4\pi}\right)^2 \left(\ln\frac{M^2}{p^2}\right)^2 . \quad (5)$$

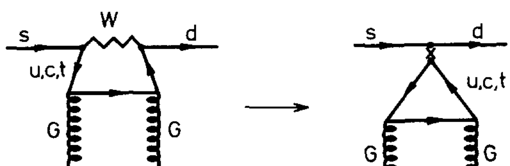


Fig. 5. The s→dGG transition reduced to a triangle diagram, when W is considered to be heavy.

The result for the double penguin can be read off (up to the factor of 1.7 from including the diagram from fig. 2) from eqs. (9), (11), (19) and (20) of ref. [3]:

$$M^{\text{DP}}_{\text{l-log}} = -\tfrac{68}{27}\,\tilde{M}_{\text{l-log}}\,. \quad (6)$$

In an analogous way we calculate the siamese penguin box

$$M^{\text{SP}}_{\text{l-log}} = (-\tfrac{32}{27} - \tfrac{3}{4}\xi)\tilde{M}_{\text{l-log}} \quad (7)$$

the diamond contribution

$$M^{\text{D}}_{\text{l-log}} = (4 - \tfrac{3}{4}\xi)\tilde{M}_{\text{l-log}} \quad (8)$$

and, finally, the mixed box

$$M^{\text{MP}}_{\text{l-log}} = (-8 + \tfrac{8}{3}\xi)\tilde{M}_{\text{l-log}}\,. \quad (9)$$

Summing up eqs. (7)–(9) proves the $\xi$ independence in the leading log approximation. Once proving this, we calculate individual diagrams in the Feynman gauge. The individual box values reported in the next section refer to this gauge.

*3. Results and conclusions.* Since the "non-leading terms" are quite sizeable in the double penguin loops [3], we proceed by considering full expressions for

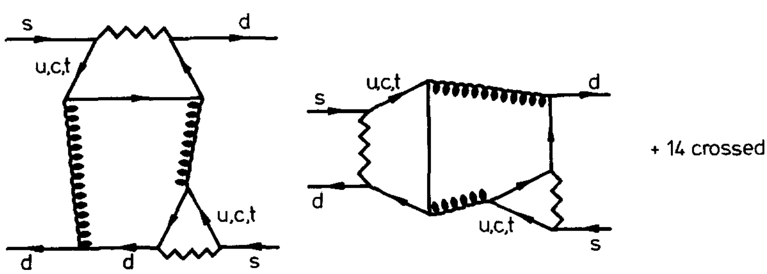


Fig. 6. Mixed penguin diagrams.

Table 1
Loop integrals entering the three terms in (11) for the choice $\mu=0.7$ GeV, $m_c=1.4$ GeV and $m_t=45$ GeV.

| Separate penguin-like box diagrams ("PL") | Loop integral | | |
|---|---|---|---|
| | *CP*-conserving $\hat{I}(\mu^2, m_c^2)$ | interference *CP*-violating $\hat{K}(\mu^2, m_t^2)$ | KM suppressed *CP*-violating $\hat{I}(m_c^2, m_t^2)$ |
| DP [a] | 12.87 | 0.58 | 13.3 |
| SP | 12.87 | 0.58 | 13.3 |
| D | 15.1 | 0.76 | 21.7 |
| MP | −82.8 | −3.62 | −79 |

[a] Note that this row is a slightly modified middle row of table 1 in ref. [3].

them. Thus, in the case of the double penguin box (which we take as a reference point), the leading-log expressions (5) and (6) get replaced by

$$-\frac{68}{27}\frac{2\sqrt{2}(G_F)^2}{16\pi^2}\left(\int dp^2[\alpha_s(p^2)^2/4\pi]^2 \times C_P(p^2, m_1^2, M_1^2)C_P(p^2, m_2^2, M_2^2)\right)(\bar{d}\gamma Ls)^2 . \quad (10)$$

The integral in (10), and the analogous integrals with the $C_P$ terms from (1) replaced by the $T$ terms from (2), determine the $K^0$–$\bar{K}^0$ mixing matrix element of the form [3]

$$\lambda_u^2 I(\mu^2, m_c^2) - 2\lambda_u\lambda_t K(\mu^2, m_t^2) + \lambda_t^2 I(m_c^2, m_t^2) , \quad (11a)$$

where we distinguish the dimensionless integrals $\hat{I}(m^2, M^2)$ defined by

$$I(m^2, M^2) = [M\alpha_s(M^2)]^2 \hat{I}(m^2, M^2) . \quad (11b)$$

In table 1 we display these integrals for the whole set of penguin-like boxes of order $\alpha_s^2 G_F^2$. In table 2 we present their individual and total contributions to the real (*CP*-conserving) and imaginary (*CP*-violating) parts of the $\Delta S=2$ mass matrix. Only the terms $\hat{I}(\mu^2, m_c^2)$ are sensitive to the infrared cut-off $\mu$. However, their contribution to the $K_L$–$K_S$ mass difference is anyhow in competition with the long distance (dispersive) effects. The most interesting loop integrals are $\hat{K}(\mu^2, m_t^2)$ and they are rather stable to both $\mu$ and $m_t$. These integrals, which are zero in the leading log approximation, give sizeable contribution in the next to leading approximation. Most of their contribution comes from the "mixed box" and can be ascribed to the coherent superposition within the biggest class of diagrams, with this particular loop structure. Then they result in the large *CP*-violating contribution which constitutes −25% of the corresponding QCD corrected [8] standard box value. By summing them up, the $\epsilon$ parameter, which comes mostly from the pure mass-matrix effect ($\epsilon \simeq \epsilon_m$) can

Table 2
Penguin-like box diagram contributions to the $\Delta S=2$ mass matrix, normalized to the double penguin box, and compared to the standard box.

| Contribution | Penguin-like box | | | | $\sum_{\text{all}}$ PL | Percentage of the QCD corrected standard box |
|---|---|---|---|---|---|---|
| | DP | SP | D | MP | | |
| *CP*-conserving | 1 | 0.47 | −0.46 | 2.52 | 3.53 | −10% |
| *CP*-violating interference | 1 | 0.47 | −0.51 | 2.45 | 3.41 | −25% |
| *CP*-violating KM suppressed | 1 | 0.47 | −0.64 | 2.32 | 3.15 | −2% |

be written in the form

$$\epsilon_m = \epsilon_{box} + \epsilon_{penguin\text{-}like} \simeq 0.75\epsilon_{box} . \quad (12)$$

In view of the remaining uncertainties [9] (the B-parameter, b-lifetime and b→u to b→c ratio), this apparent reduction of the value given by the standard box still does not mean the inconsistency between the experimental and theoretical values of $\epsilon$. Moreover, the message of our paper is that before claiming to have such inconsistencies, more accurate calculations within the standard model are also needed. In particular, we have shown here the importance of additional loops for an effect (*CP* violation) which is genuinely a loop effect. The loops in question are double penguin-like boxes of order $\alpha_s^2 G_F^2$, different from the order $\alpha_s^2$ QCD corrected ordinary box. The way in which we incorporate QCD effects, by putting $\alpha_s \to \alpha_s(p^2)$ under the loop integrals, is inspired by previous loop calculations [10,11]. The role of double penguin loops in predicting the *CP*-violating parameter $\epsilon$ is rather evident since there are no uncertainties due to long-distance physics in this case. We end up with the SD, $\Delta S = 2$ local four-quark hamiltonian. The ratio of its matrix element to the standard box one is free of ambiguities.

We thank Roberto Peccei for reading the manuscript and for useful comments. We also thank Fernando Cornet for providing us with a convenient numerical routine.

## *References*

[1] D. Hochberg and R.G. Sachs, Phys. Rev. D 27 (1983) 606.
[2] G. Ecker, Phys. Lett. B 147 (1984) 369.
[3] J.O. Eeg and I. Picek, Phys. Lett. B 160 (1985) 154.
[4] P. Langacker, UPL-0288T preprint (1985); I. Picek, DESY 86-36 preprint.
[5] M.K. Gaillard and B.W. Lee, Phys. Rev. D 10 (1974) 897.
[6] J.O. Eeg and I. Picek, Nucl. Phys. B 244 (1984) 77; Phys. Lett. B 130 (1983) 308.
[7] J.F. Donoghue, E. Golowich and G. Valencia, UMHEP-234 preprint.
[8] F.J. Gilman and M.B. Wise, Phys. Rev. D 27 (1983) 1128.
[9] R.D. Peccei, DESY 85-121 preprint.
[10] A.I. Vainshtein, V.I. Zakharov, V.A. Novikov and M.A. Shifman, Yad. Fiz. 23 (1976) 1024 [Sov. J. Nucl. Phys. 23 (1976) 540]; Phys. Rev. D 16 (1977) 223.
[11] J.O. Eeg, Phys. Rev. D 23 (1981) 2596.